Numerical Simulation of Supersonic Combustion of Pylon Injected Hydrogen Fuel in Scramjet Combustor

A Javed, *Non-member*
D Chakraborty, *Non-member*

Combustion process in a hydrogen fuelled Scramjet combustor has numerically been studied. Hydrogen is injected at sonic speed in supersonic air stream from a pylon type of injector at 120° from the airflow. The supersonic airstream is at Mach number of 2.15 and total temperature of 1350 K. The 3-D Navier Stokes equations with Shear Stress Transport (SST) turbulence model are solved using commercial Computational Fluid Dynamics (CFD) software CFX-TASC Flow. Combustion is modelled using multi-step Eddy Dissipation Model (EDM) with seven species and five reactions. A good match is obtained for wall static pressure distribution with multi-step chemistry which could be obtained with single-step chemistry.

Keywords : Numerical simulation; Supersonic combustion; Hydrogen fuel; Scramjet combustor

NOTATION

a_l	:	modelling constant
D	:	molecular diffusion coefficient
F_1, F_2	:	blending functions
h	:	static enthalpy
H	:	total enthalpy
J	:	diffused species mass
k	:	turbulent kinetic energy
P	:	pressure
P_k	:	production term
Pr_t	:	turbulent Prandtl number
R	:	gas constant
R_k	:	species production
S	:	strain rate
Sc_t	:	turbulent Schmidt number
t	:	time
T	:	temperature
u	:	velocity
x	:	distance
Y_m	:	mass fraction of mth species

Greek Symbols

$\alpha_1, \alpha_2, \alpha_3$	:	modelling constants
β^*	:	modelling constant
$\beta_1, \beta_2, \beta_3$	:	modelling constant
δ_{ij}	:	kronecker delta
λ	:	thermal conductivity
μ	:	dynamic viscosity
ν_t	:	kinematic eddy viscosity
ρ	:	density
$\sigma_{k1}, \sigma_{k2}, \sigma_{k3}$	:	modelling constants
$\sigma_{\omega1}, \sigma_{\omega2}, \sigma_{\omega3}$	:	modelling constants
Φ	:	modelling constant
ω	:	inverse time scale of eddy dissipation

Suffix

i, j, k, l	:	directions
eff	:	effective
m	:	m^{th} species

Superscripts

~	:	Favre averaged value
—	:	time averaged value

A Javed and D Chakraborty are with The Computational Combustion Dynamics Division of the Defence Research and Development Laboratory, Kanchanbagh, Hyderabad 500 058.

INTRODUCTION

Fundamental to the success of the development of advanced airbreathing propulsion system capable of sustaining hypersonic flight in the atmosphere is the ability to understand the mixing and combustion process in the combustor. For efficient combustion, it is necessary to produce homogeneous fuel/air mixture rapidly across the whole combustor. Experimental and numerical data[1,2] show that fuel injection from the wall will result in reaction zones that occupy only a small fraction of the flow field. Therefore, not all of the oxygen supplied by the air stream entering the combustor can participate in the chemical reaction. Furthermore, the reaction zones close to the wall will exert excessive thermal loads on the structure of the combustor. This problem of slow lateral fuel transport in the airstream can be circumvented by injecting the fuel in the centre of the flow by means of pylon. Various pylon designs have been investigated experimentally[3,4] to study their effectiveness in fuel mixing and combustion in the Scramjet combustor. Numerical

simulation of the reacting flow field for pylon injected hydrogen fuel in the Scramjet combustor is very limited.

Reacting flow field of Scramjet combustor for pylon injected hydrogen fuel is reported in this study. The experimental condition of Gruenig, et al [3] has been simulated numerically and the computational results are compared with the experimental values.

METHODOLOGY

Computational Fluid Dynamics (CFD) software CFX-TASCFlow is used for the present analysis. It is a fully implicit 3-D Navier-Stokes code, capable of solving diverse and complex turbulent reacting fluid flow problems. The code implements a general non-orthogonal, structured, boundary fitted grids[5].

Governing Equations

Most of the high speed combustion applications can be described as chemically reacting single phase multi species flows. The basic governing equations for such flows are Navier-Stokes equation coupled with $(n\text{-}1)$ species mass continuity equations (n is the number of species considered). The Favre averaged form of these equations is written as follows.

Continuity

$$\frac{\partial \bar{\rho}}{\partial t} + \frac{\partial}{\partial x_j}\left(\bar{\rho}\,\tilde{u}_j\right) = 0$$

Momentum

$$\frac{\partial}{\partial t}\left(\bar{\rho}\,\tilde{u}_i\right) + \frac{\partial}{\partial x_j}\left(\bar{\rho}\,\tilde{u}_i\tilde{u}_j\right) = -\frac{\partial \bar{P}}{\partial x_j} + \frac{\partial}{\partial x_j}\left(\mu_{\text{eff}}\left(\frac{\partial \tilde{u}_i}{\partial x_j} + \frac{\partial \tilde{u}_j}{\partial x_i}\right) - \frac{2}{3}\mu_{\text{eff}}\left(\frac{\partial \tilde{u}_l}{\partial x_l}\right)\delta_{ij}\right)$$

where

$$\mu_{\text{eff}} = \mu + \mu_t$$

here μ_t is a modelling constant and is known as eddy viscosity. It is further discussed in turbulence modelling.

Energy

$$\frac{\partial}{\partial t}\left(\bar{\rho}\tilde{H}\right) - \frac{\partial \bar{P}}{\partial t} + \frac{\partial}{\partial x_j}\left(\bar{\rho}\tilde{H}\tilde{u}_j\right) = \frac{\partial}{\partial x_j}\left(\lambda\frac{\partial \tilde{T}}{\partial x_j} + \frac{\mu_t}{\text{Pr}_t}\frac{\partial \tilde{h}}{\partial x_j}\right) + \frac{\partial}{\partial x_j}\left(\tilde{u}_i\left(\mu_{\text{eff}}\left(\frac{\partial \tilde{u}_i}{\partial x_j} + \frac{\partial \tilde{u}_j}{\partial x_i}\right) - \frac{2}{3}\mu_{\text{eff}}\left(\frac{\partial \tilde{u}_l}{\partial x_l}\right)\delta_{ij}\right) + \mu\frac{\partial k}{\partial x_j}\right)$$

Species Conservation

$$\frac{\partial}{\partial t}\left(\bar{\rho}\tilde{Y}_m\right) + \frac{\partial}{\partial x_j}\left(\bar{\rho}\tilde{Y}_m\tilde{u}_j\right) = R_{k,m} - \frac{\partial}{\partial x_j}\left(\tilde{J}_j + \frac{\mu_t}{\text{Sc}_t}\frac{\partial \tilde{Y}_m}{\partial x_j}\right)$$

where

$$\tilde{J}_j = -\bar{\rho}D\frac{\partial \tilde{Y}_m}{\partial x_j}$$

Apart from these equations, equation of state is used to close the system of equations

$$\bar{P} = \bar{\rho}\,R(\tilde{Y}_m)\tilde{T}$$

Turbulence Modelling

Turbulence is modelled using Menter's Shear Stress Transport (SST) model[6]. The SST turbulence model is derived by blending $k\text{-}\omega$ model applied to the inner portion of the turbulent boundary layer with a high Reynolds number form of the k - $\in$ turbulence model transformed into the k and ω variables being applied to the outer portion of the turbulent boundary layer. A parameter F_1 is defined so as to equal one for the near wall region and to vary smoothly to zero as the outer region of the turbulent boundary layer is reached. By assigning a weight of F_1 to the inner k - ω model and a weight of $(1\text{-}F_1)$ to the outer transformed k - ε model, advantages of both models are incorporated into the new SST model. Additionally, the eddy viscosity relation is modified to provide a lag in development of the eddy viscosity for strong interaction flows. Both the model equations are given as follows.

Original k-ω Model

$$\frac{\partial\left(\bar{\rho}k\right)}{\partial t} + \frac{\partial\left(\bar{\rho}\tilde{u}_jk\right)}{\partial x_j} = P_k - \beta^*\bar{\rho}k\omega + \frac{\partial}{\partial x_j}\left[\left(\mu + \frac{\mu_t}{\sigma_{k1}}\right)\frac{\partial k}{\partial x_j}\right]$$

$$\frac{\partial\left(\bar{\rho}\omega\right)}{\partial t} + \frac{\partial\left(\bar{\rho}\tilde{u}_j\omega\right)}{\partial x_j} = \alpha_1\frac{\omega}{k}P_k - \beta_1\bar{\rho}\omega^2 + \frac{\partial}{\partial x_j}\left[\left(\mu + \frac{\mu_t}{\sigma_{\omega1}}\right)\frac{\partial \omega}{\partial x_j}\right]$$

Transformed k-ε Model

$$\frac{\partial\left(\bar{\rho}k\right)}{\partial t} + \frac{\partial\left(\bar{\rho}\tilde{u}_jk\right)}{\partial x_j} = P_k - \beta^*\bar{\rho}k\omega + \frac{\partial}{\partial x_j}\left[\left(\mu + \frac{\mu_t}{\sigma_{k2}}\right)\frac{\partial k}{\partial x_j}\right]$$

$$\frac{\partial\left(\bar{\rho}\omega\right)}{\partial t} + \frac{\partial\left(\bar{\rho}\tilde{u}_j\omega\right)}{\partial x_j} = \alpha_2\frac{\omega}{k}P_k - \beta_2\bar{\rho}\omega^2 + \frac{\partial}{\partial x_j}\left[\left(\mu + \frac{\mu_t}{\sigma_{\omega2}}\right)\frac{\partial \omega}{\partial x_j}\right] + 2\bar{\rho}\sigma_{\omega2}\frac{1}{\omega}\frac{\partial k}{\partial x_j}\frac{\partial \omega}{\partial x_j}$$

Now the first two equations for $k\text{-}\omega$ model are multiplied by function F_1 and the equations for $k\text{-}\in$ model are multiplied by a function $(1\text{-}F_1)$ and the corresponding $k\text{-}$ and ω-equations are added to give the following equations

$$\frac{\partial\left(\bar{\rho}k\right)}{\partial t} + \frac{\partial\left(\bar{\rho}\tilde{u}_jk\right)}{\partial x_j} = P_k - \beta^*\bar{\rho}k\omega + \frac{\partial}{\partial x_j}\left[\left(\mu + \frac{\mu_t}{\sigma_{k3}}\right)\frac{\partial k}{\partial x_j}\right]$$

$$\frac{\partial\left(\bar{\rho}\omega\right)}{\partial t} + \frac{\partial\left(\bar{\rho}\tilde{u}_j\omega\right)}{\partial x_j} = \alpha_3\frac{\omega}{k}P_k - \beta_3\bar{\rho}\omega^2 + \frac{\partial}{\partial x_j}\left[\left(\mu + \frac{\mu_t}{\sigma_{\omega3}}\right)\frac{\partial \omega}{\partial x_j}\right] +$$

$$\left(1 - F_1\right)2\bar{\rho}\sigma_{\omega2}\frac{1}{\omega}\frac{\partial k}{\partial x_j}\frac{\partial \omega}{\partial x_j}$$

·The production term is given as

$$P_k = \mu_t \left(\frac{\partial \tilde{u}_i}{\partial x_j} + \frac{\partial \tilde{u}_j}{\partial x_i} \right) \frac{\partial \tilde{u}_i}{\partial x_j} - \frac{2}{3} \delta_{ij} \left(\overline{\rho} k + \mu_t \frac{\partial \tilde{u}_k}{\partial x_k} \right) \frac{\partial \tilde{u}_i}{\partial x_j}$$

The coefficients of the new model are a linear combination of the corresponding coefficients of the underlying models.

$$\Phi_3 = F_1 \Phi_1 + (1 - F_1) \Phi_2$$

All coefficients are listed below

α_1	=	5/9
α_2	=	0.44
β_1	=	3/40
β_2	=	0.0828
β^*	=	0.09
σ_{k1}	=	2
$\sigma_{\kappa 2}$	=	1
$\sigma_{\omega 1}$	=	2
$\sigma_{\omega 2}$	=	0.856

The proper transport behaviour to predict separation is obtained by a limiter to the formulation of eddy viscosity. This is given as follows

$$\nu_t = \frac{a_1 k}{\max(a_1 \omega, \ S \ F_2)}$$

and

$$\mu_t = \overline{\rho} \nu_t$$

Again F_2 is a blending function similar to F_1, which restricts the limiter to the wall boundary layer, as the underlying assumptions are not correct for free shear flows. S is an invariant measure of the strain rate as given below. The constant a_1 is equal to 0.31.

$$S = \sqrt{\left(\frac{\partial \tilde{u}_i}{\partial x_j} + \frac{\partial \tilde{u}_j}{\partial x_i} \right) \frac{\partial \tilde{u}_i}{\partial x_j}}$$

Blending Functions

The blending functions are critical to the success of the method. Their formulation is based on the distance to the nearest surface and on the flow variables

$$F_1 = \tanh\left(arg_1^4 \right)$$

with

$$arg_1 = \min\left\{ \max\left(\frac{\sqrt{k}}{\beta^* \omega y}; \ \frac{500\nu}{y^2 \omega} \right); \ \frac{4\rho \sigma_{\omega 2} k}{CD_{k\omega} y^2} \right\}$$

and

$$CD_{k\omega} = \max\left(2\rho \sigma_{\omega 2} \frac{1}{\omega} \frac{\partial k}{\partial x_j} \frac{\partial \omega}{\partial x_j}, \ 1.0 \times 10^{-10} \right)$$

$$F_2 = \tanh\left(arg_2^2 \right)$$

with

$$arg_2 = \max\left(2 \frac{\sqrt{k}}{\beta^* \omega y}; \ \frac{500\nu}{y^2 \omega} \right)$$

Kato Launder Correction

In a stagnation flow, the very high levels of S produce excessive levels of turbulent kinetic energy[7] whereas deformation near stagnation point is almost irrotational. The production term

$$P_k = \mu_t S^2 - \frac{2}{3} \delta_{ij} \left(\overline{\rho} k + \mu_t \frac{\partial \tilde{u}_k}{\partial x_k} \right) \frac{\partial \tilde{u}_i}{\partial x_j} \quad \text{is modified as}$$

$$P_k = \mu_t S \Omega - \frac{2}{3} \delta_{ij} \left(\overline{\rho} k + \mu_t \frac{\partial \tilde{u}_k}{\partial x_k} \right) \frac{\partial \tilde{u}_i}{\partial x_j}$$

where

$$\Omega = \sqrt{\left(\frac{\partial \tilde{u}_i}{\partial x_j} - \frac{\partial \tilde{u}_j}{\partial x_i} \right) \frac{\partial \tilde{u}_i}{\partial x_j}}$$

This leads to marked reduction in energy production near stagnation point while having no effect in a simple shear flow.

Combustion Modelling

Combustion is modelled with Multi-step Eddy Dissipation Model (EDM). In a multi-reaction model, the challenge is to define the minimum number of reactions necessary to represent the important characteristics of the flame. A two-step process involving partial conversion of fuel to intermediate species with complete conversion to products in a second step is often employed. More steps are added to capture mechanisms occurring in the flame under non-stoichiometric conditions. In the present case, the following set of reactions are chosen for hydrogen combustion in air:

$$H_2 + O_2 = 2OH$$
$$H_2 + OH = H_2O + H$$
$$H + OH = H_2O$$
$$H + O_2 = OH + O$$
$$H_2 + O = H_2O$$
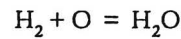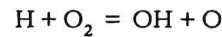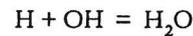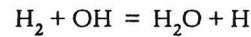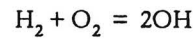
The rate of any reaction may be limited by kinetics or by physical mixing. The physical mixing describes the process of generating a homogeneous mixture of reactants at the molecular level. Kinetics describes the rate at which molecules collide with sufficient energy to react. Both of these processes are essential for reaction to occur and either one may control the overall progress of the reaction. Thus, the slower of the mixing and kinetic process is assumed to be rate determining.

In CFX-TASC Flow, each reaction may contain up to two reactants and two products. The k th reaction is represented by

$$\text{fuel}_k + r_k \ \text{oxidant}_k = f_k(1 + r_k) \ \text{product1}_k + (1 - f_k)(1 + r_k) \ \text{product2}_k$$

3
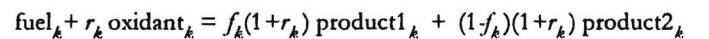
where r_k is the mass stoichiometry of the kth reaction and f_k is the mass fraction of product which is the first product (mass first product/ total mass products).

The mixing rate determined from the Eddy Dissipation Model (EDM) is given as

$$R_{k, edm} = -A_{ebu}\bar{\rho}\frac{\varepsilon}{k}\min\left\{Y_f, \frac{Y_o}{r_k}, B_{ebu}\frac{Y_p}{1 + r_k}\right\}$$

where Y_f is the mass fraction of fuel; Y_o, the mass fraction of oxidant; Y_p, the mass fraction of products; A_{ebu}, the model constant, and B_{ebu} is also the model constant.

A single mixing rate constant, (A_{ebu}), is used to relate the characteristic turbulent mixing rate (ε/k) to the reaction rate. In multi-step EDM, the product limitation is, by default, switched off.

The kinetic rate of change of any species in a reaction is generally described by an Arrhenius expression involving an exponential dependence on temperature and a power law dependence on the concentrations of the reacting chemical species

$$R_{k, kin} = -A_c T^\beta [C_a]^n [C_b]^m \exp\left(-\frac{E_T}{T}\right)$$

where A_c is the pre-exponential factor; β, the temperature exponent; C_j, the concentration of reactant, and E_T is the activation temperature of the reaction.

Other forms may be appropriate depending on the reaction. For example, it is common to have concentration dependencies for gas species other than those involved in the reaction.

The rate of the reaction is then determined from the minimum of the mixing and kinetic rate and is expressed as

$$R_k = \min\left(R_{k, edm}, R_{k, kin}\right)$$

The source term for each species is finally determined from the sum of the change in that species from all reactions.

RESULTS AND DISCUSSION

Fuel injection with pylon type injectors has been studied experimentally by Gruenig, et al [3]. Performance of various pylon injector configurations in the scramjet combustor has been evaluated experimentally in a connect pipe mode test, with respect to pressure rise in the combustor. The combustor used for these tests is 645-mm long, 25-mm wide, and its height is 27.5 mm at the entry and 40.5 mm at the exit. The pylon is placed at a distance of 45-mm from the combustor entry. An expansion angle of 5° is provided on the lower surface of the combustor for 150 mm just after the pylon. This expansion caters for the decrease in Mach number due to heat addition. Rest of the combustor is a straight duct after this expansion portion. Although four different pylon designs are studied experimentally [3], the present study deals with numerical investigation of only one pylon configuration. Height of this pylon is 10 mm. Hydrogen is injected at a total pressure of 39 bar at 120° angle to the airflow from slot shaped orifice at sonic speed. The area of the slot shaped orifice is equivalent to a 1.28-mm dia circular hole. Vitiated air at a Mach number of 2.15, total temperature 1350 K and

total pressure 7.8 bar enters into the combustor. The mass fraction of oxygen in this vitiated air is 0.193, whereas the mass fractions of nitrogen and water vapour are 0.727 and 0.080, respectively. The experimental conditions correspond to free stream Mach number of 6.5 and altitude 23.5 km. Summary of different flow parameters for both hydrogen and air stream considered for simulation is given in Table 1.
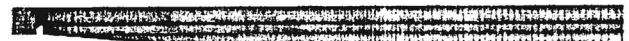
The combustor geometry with the grid structure is shown in Figure 1. The grid structure near the pylon is also shown in Figure 1. Taking the advantage of the symmetry, only one half of the geometry is simulated. A total of 0.18 million grid is employed in the flow field. The grid is fine near the pylon and near wall region while the grid is relatively coarse in other regions.

The reacting flow field in the scramjet combustor has been simulated by solving 3-D Navier Stokes equations with SST turbulence model using commercial CFD Software CFX-TASC Flow [5]. Kato Launder correction in the production term of the turbulent kinetic energy equation for stagnation effects on turbulence is also incorporated in this software. Turbulence chemistry interaction is modelled by five equations, seven species, multi-step eddy dissipation model as discussed in the methodology section.

Qualitative feature of the flow field is presented through the pressure distribution in the plane of symmetry. The shock reflections in the combustor are clearly visible in Figure 2. The appearance of bow shock caused due to the injection is also seen in Figure 2. Mach number distributions in the plane of injector for the reacting and non-reacting cases are shown in Figure 3. For the non-reacting case,

Table 1 Different flow parameters for air and hydrogen

Parametre	m, kg/s	T_0, K	M	P_0, bar	U, m/s	Re
Air	0.3300	1350	2.15	7.8	1190	4.6×10^5
H$_2$ Jet	0.0032	280	1.00	39.0	1160	9.3×10^5

Geometry of combustor with the grid

Blown up view near the pylon

Figure 1 Combustor geometry with the grid structure

Blown up view near the pylon

5.0×10^4 Pa 2.7×10^5 Pa 5.0×10^5 Pa

Figure 2 Pressure distribution in the plane of symmetry

.the low speed region is confined to the wake region of pylon, whereas for the reacting case significant reduction of Mach number is visible in the reaction zone in the combustor.

Hydrogen mass fraction distribution is shown in Figure 4. The reduction in hydrogen mass fraction along the length of combustor can be clearly seen. This reduction in mass fraction of hydrogen occurs due to diffusion and combustion.

The combustor surface pressure distribution at the upper wall for the reacting case is shown in Figure 5. A reasonable good match has been obtained between the computational and experimental values. The shock reflections in the combustor also confirm the presence of supersonic flow in the combustor. The computed surface pressure

comparison between reacting and non-reacting case is shown in Figure 6. Significant increase in the pressure is seen for the reacting case due to combustion in supersonic stream.

Results of a single step chemistry simulation were compared with the multi-step chemistry simulation results. The single step used is the combination of hydrogen and oxygen to give water. The comparison of surface static pressures is shown in Figure 7. From Figure 7, it can be observed that the pressure rise with single step chemistry does not match with the experimental points, and is much higher compared to the multi-step chemistry results. Near the fuel injection point, due to injection direction and high speed of incoming air, the mixing of fuel and air is very good. This good mixing coupled with single step
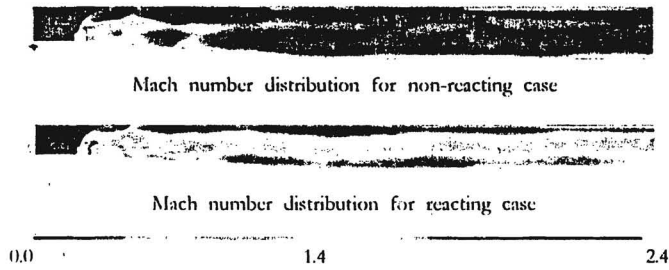

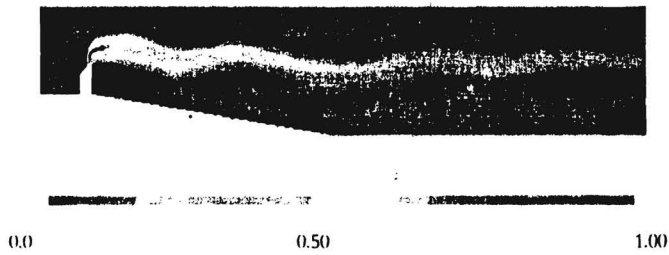Figure 3 Mach number distribution in the plane of symmetry

Figure 4 Hydrogen mass fraction distribution in the plane of symmetry

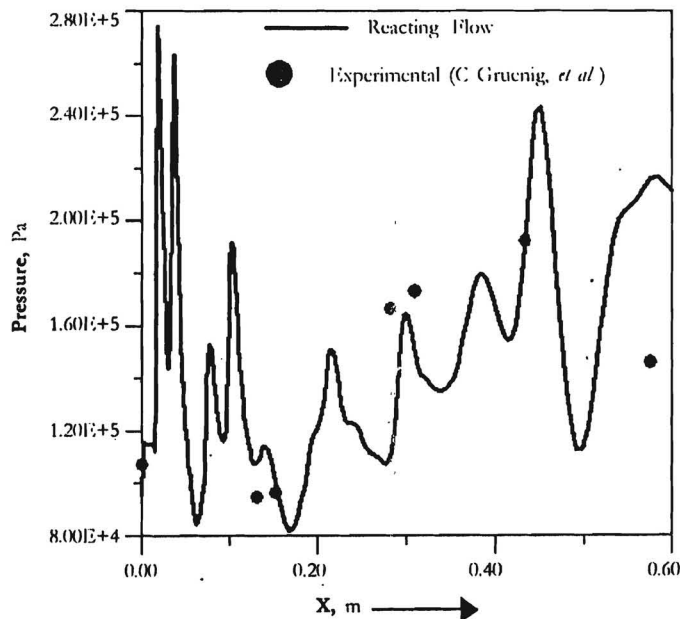Figure 5 Computational and experimental surface pressure distribution
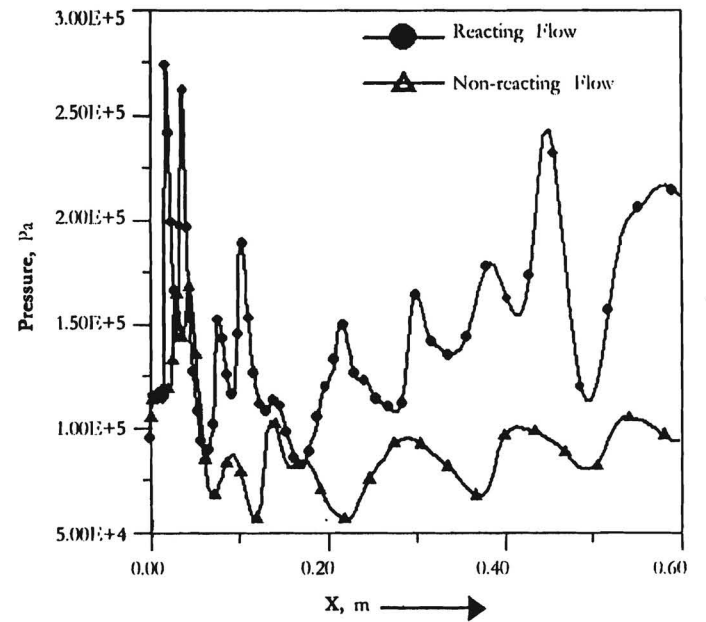

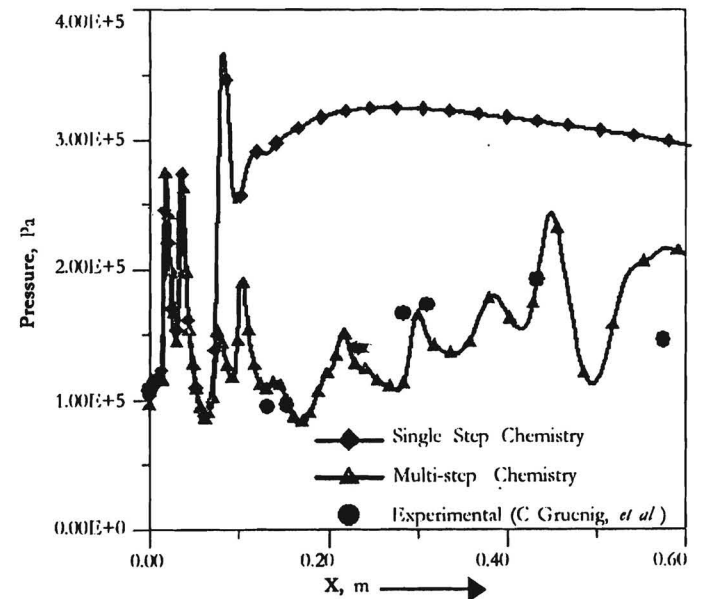Figure 6 Computational surface pressure distribution for reacting and non-reacting flow

Figure 7 Computational of single step and multi-step chemistry results

reaction liberates all the heat of combustion of fuel as soon as it meets oxidiser. The heat released near the injection location is very high. This high rate of heat release causes a strong pre combustion shock to form and complete flow field becomes subsonic, and rest of the heat is added at subsonic speeds as can be observed from Figure 7. The single step chemistry static pressure drops slowly due to heat addition in subsonic mode after the pre combustion shock peak.

CONCLUSION

Scramjet combustor flow field for pylon injected hydrogen fuel has been investigated numerically by solving 3-D Navier Stokes equations with SST turbulence model using commercial CFD Software CFX-TASC Flow. Turbulence chemistry interaction is modelled by a multi-step eddy dissipation model. The simulation captures all the essential features of the flow field including the shock reflection in the combustor and the occurrence of bow shock ahead of injection. An extensive reaction zone has been obtained causing a significant rise of surface pressure in the combustor. The computed surface pressure matches reasonably well with the experimental values. The software can be used as an efficient design tool for the design and development of pylon-based Scramjet combustor.

REFERENCES

1. J D Abbitt, R J Hartfield and J C Mc Dannej. 'Mole Fraction Imaging of Transverse Injection in a Ducted Supersonic Flow'. *AIAA Journal*, vol 29 no 3, 1991, p 431.

2. K Yokota and S Kaji. "Two and Three Dimension Study on Supersonic Flow and Mixing Fields with Hydrogen Injection'. *AIAA Paper 95-6024*, 1995

3. C Gruenig, V Avrashkov and F Mayinger. 'Fuel Injection into a Supersonic Airflow by Means of Pylons'. *Journal of Propulsion and Power* vol 16, no 1, 2000, p 29.

4. C Gruenig, V Avrashkov and F Mayinger. 'Self-Ignition and Supersonic Reaction of Pylon-Injected Hydrogen Fuel'. *Journal of Propulsion and Power* vol 16, no 1, 2000, p 35.

5. CFX-TASC Flow Computational Fluid Dynamics Software (Version 2.11.1). *AEA Technology Engineering Software Ltd*, 2001.

6. F R Menter. "Two - Equation Eddy - Viscosity Turbulence Models for Engineering Applications'. *AIAA Journal*, vol 32, no 8, August 1994, p 1598

7. M Kato and B E Launder. "The Modelling of Turbulent Flow Around Stationary and Vibrating Square Cylinders'. *Proceedings of the Ninth Symposium on Turbulent Shear Flows*, Japan, vol 9, 1993, p 10-4-1.